Research Square

Preprints are preliminary reports that have not undergone peer review.
They should not be considered conclusive, used to inform clinical practice,
or referenced by the media as validated information.

Remote N-Substituent-Tuned Dichotomous Diradical Scission Enables Photocatalytic Divergent Rearrangement of Allylic Aminophosphines

Bing Han

hanb@lzu.edu.cn

Lanzhou University https://orcid.org/0000-0003-0507-9742

Peng-Fei Zhao

Lanzhou University

Zuo-Shuai Wang

Lanzhou University

Hao Chen

Lanzhou University

Long-Yu Xing

Lanzhou University

Article

Keywords:

Posted Date: November 6th, 2026

DOI: https://doi.org/10.21203/rs.3.rs-11490780/v1

License: This work is licensed under a Creative Commons Attribution 4.0 International License.
Read Full License

Additional Declarations: There is **NO** Competing Interest.

Remote N-Substituent-Tuned Dichotomous Diradical Scission Enables Photocatalytic Divergent Rearrangement of Allylic Aminophosphines

Peng-Fei Zhao[§], Zuo-Shuai Wang[§], Hao Chen, Long-Yu Xing & Bing Han*

State Key Laboratory of Natural Product Chemistry, College of Chemistry and Chemical Engineering, Lanzhou University, Lanzhou, China.

E-Mail: hanb@lzu.edu.cn

[§] These authors contributed equally to this work.

Abstract:

Organophosphorus compounds are widely prevalent in pharmaceuticals, agrochemicals, and functional materials, and phosphoranyl radicals represent a versatile platform for the construction of these valuable molecules. Although the selectivity of α- and β-scission dictates the reaction outcomes of phosphoranyl radical transformations, established strategies for tuning such fragmentation are confined to monoradical systems and rely on local structural modification at the phosphorus center. Herein, we realize remote N-substituent-controlled switching between α- and β-scission pathways of phosphorus–carbon triplet diradicals and apply this concept in a visible-light energy transfer photocatalytic divergent rearrangement of allylic aminophosphines to access two structurally significant organophosphorus skeletons. Computational studies reveal that the electronic properties of N-substituents govern the geometries of phosphoranyl radicals: N-alkoxy substituents favour α-scission, whereas N-sulfonyl substituents promote β-scission. This work provides new mechanistic insights into heteroatom diradical reactivity and broadens the available tools for divergent synthesis of organophosphorus compounds.

Introduction

Organic radicals, unique open-shell intermediates, are key active species for the construction and deconstruction of chemical bonds and molecular skeletons in modern synthetic chemistry.[1,2] Among them, bond-forming elementary reactions such as radical addition and cyclization are well-established, and their selectivity control has been extensively explored.[3-7] In contrast, the elementary radical fragmentation reactions including α- and β-scission, which enable selective bond cleavage and dominate radical rearrangement[8-14] and skeleton reorganization,[15-19] remain challenging with respect to the precise modulation of fragmentation selectivity. Conventional radical fragmentation follows fixed single reactivity modes. For instance, boron-, carbon-, nitrogen- and oxygen-centred organic radicals,[20-24] owing to their intrinsic electronic structures, possess only β-scission as the dominant pathway, enabling merely site-selective control among different β-bonds according to bond dissociation energy (BDE). By contrast, hypervalent silicon radicals prefer α-scission and only allow site optimization within a single α-scission manifold.[25-26] None of these systems can achieve competitive switching between discrete α- and β-scission pathways.

Among organic radicals, phosphoranyl radicals feature competing low-energy α- and β-scission channels with well-matched energies, making them ideal platforms for selectivity modulation.[27] Their fragmentation selectivity has long been investigated,[28–30] supporting access to unique

organophosphorus compounds[31–35] and new radical transformations.[36–39] Prior studies show that α/β-scission selectivity of alkoxy-, alkylthio- and aminophosphoranyl radicals is primarily governed by BDEs and radical stability (Figure 1a). Doyle and Hong's recent advances further broadened phosphoranyl radical chemistry: tuning phosphine skeletons allowed selective α-scission and β-scission of aminophosphoranyl radicals, respectively,[40–42] delivering alkene aminohydrogenation and sulfonylfunctionalization methods (Figure 1b). While switchable dual scission has been achieved, all known systems are limited to monoradicals, and regulable scission of phosphoranyl-based diradicals remains unreported (Figure 1c). Moreover, existing selectivity regulations rely entirely on structural modification at the α-position of the P-center, whereas a dichotomous scission system precisely modulated by remote substituent electronic effects has not yet been documented. Thus, exploiting remote electronic effects to balance α-scission and β-scission of heteroatom-containing triplet diradicals offers new mechanistic understanding of radical fragmentation and enables divergent radical rearrangement and skeleton reconstruction.

Motivated by the aforementioned bottlenecks and our long-standing interest in phosphine rearrangements,[43,44] we sought to develop a dual-channel scission reaction of phosphoranyl radical-based diradicals precisely regulated by remote electronic effects. We aimed to realize the first radical scission-controlled divergent rearrangement, enabling the modular synthesis of structurally diverse and synthetically valuable organophosphorus compounds. Enabled by visible-light energy transfer (EnT) photocatalysis,[45-53] we hypothesized that the styrene moiety of allylic aminophosphines could be excited to the corresponding carbon-centered diradicals, which undergo cyclization onto the P(III) center to furnish a key triplet phosphorus-carbon diradical intermediate. This intermediate bears both carbon- and phosphoranyl-radical active sites and is expected to break the established reactivity patterns of conventional phosphoranyl radicals. We envisioned that electron-donating or electron-withdrawing effects from remote N-substituents can tune the geometry of the phosphoranyl radical center to switch scission selectivity by modulating the SOMO energy level. That is, the strong electron-donating character of the N-methoxy group would lead to a higher-energy, localized SOMO of the phosphoranyl radical and thus afford a trigonal bipyramidal geometry at the P centre, where the unpaired electron occupies an apical site.[54] This structural preference favours α-scission to generate a trivalent phosphorus-substituted aziridine. In contrast, strong electron-withdrawing substituents such as N-tosyl would lead to a lower-energy, delocalized counterpart and thus reshape its configuration into a square pyramidal geometry, where the unpaired electron resides at an equatorial position via partial N-P interaction.[55] This structural preference favours β-scission to generate a carbon-centered diradical, ultimately affording the rearrangement product N-sulphonyl diphenyl(2-phenylallyl)-λ^5-phosphanimine (Figure 1c).

Guided by this hypothesis, we prepared allylic aminophosphines in situ via condensation of N-substituted allylic amines with R_2PCl. Using visible-light EnT catalysis, we realized the first divergent phosphorus-skeleton rearrangement controlled by diradical scission to access synthetically useful organophosphorus products (Figure 1d). Given the broad utility of organophosphorus frameworks in pharmaceuticals, agrochemicals and functional materials, this strategy enables modulation of competing radical scission pathways and facile construction of diverse organophosphorus compounds.[56–58] Distinct from prior approaches that modify the phosphorus center locally, this work establishes a new diradical regulation principle: remote electronic effects dictate the competition between α- and β-scission of heteroatom-containing triplet diradicals. This method allows switchable assembly of two distinct phosphorus skeletons and

expands the toolbox of phosphorus radical rearrangement chemistry. The findings provide mechanistic insights into controllable heteroatom diradical transformations and inspire new divergent rearrangement designs.

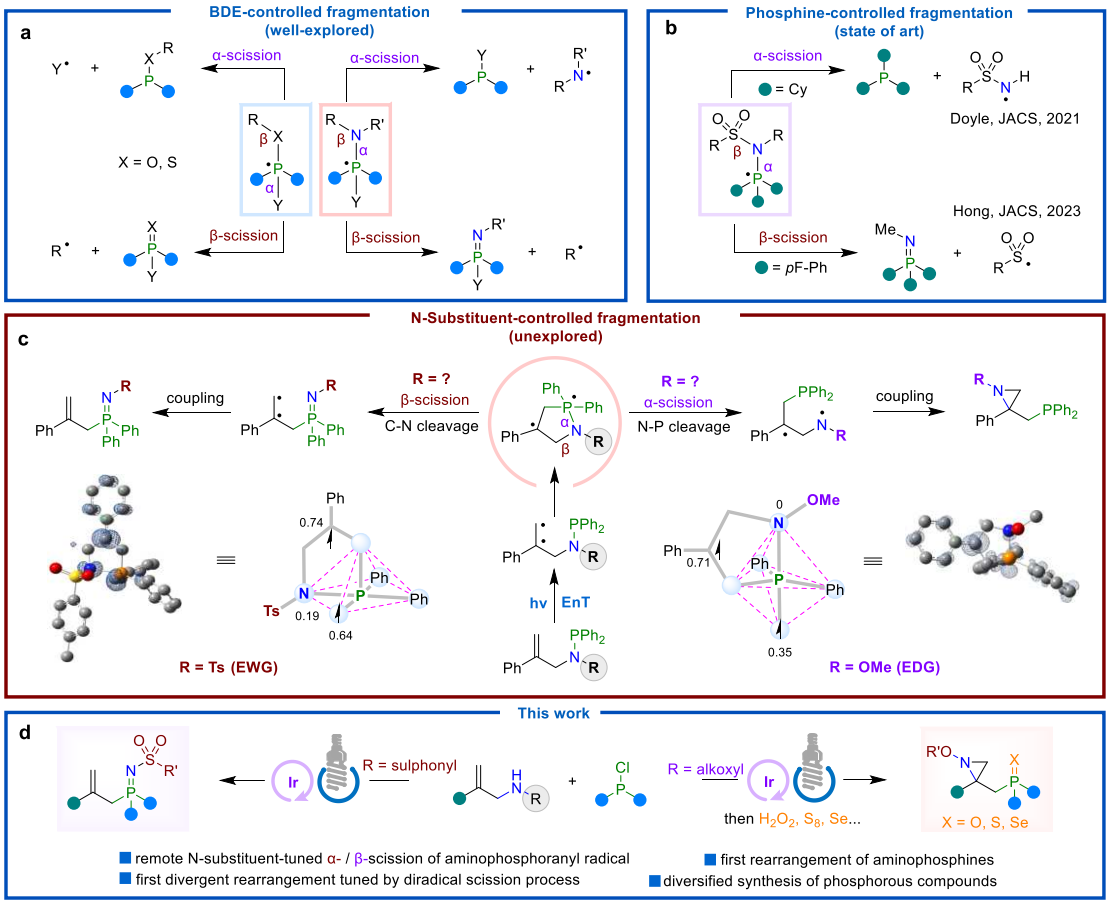


Figure 1. Fragmentation and Applications of Phosphoranyl Radicals. (a) Conventional phosphoranyl radical fragmentation. (b) Phosphine-controlled aminophosphoranyl radical fragmentation. (c) N-substituent-controlled dichotomous diradical scission, configuration analysis and spin distribution map. (d) Divergent rearrangement of aminophosphines.

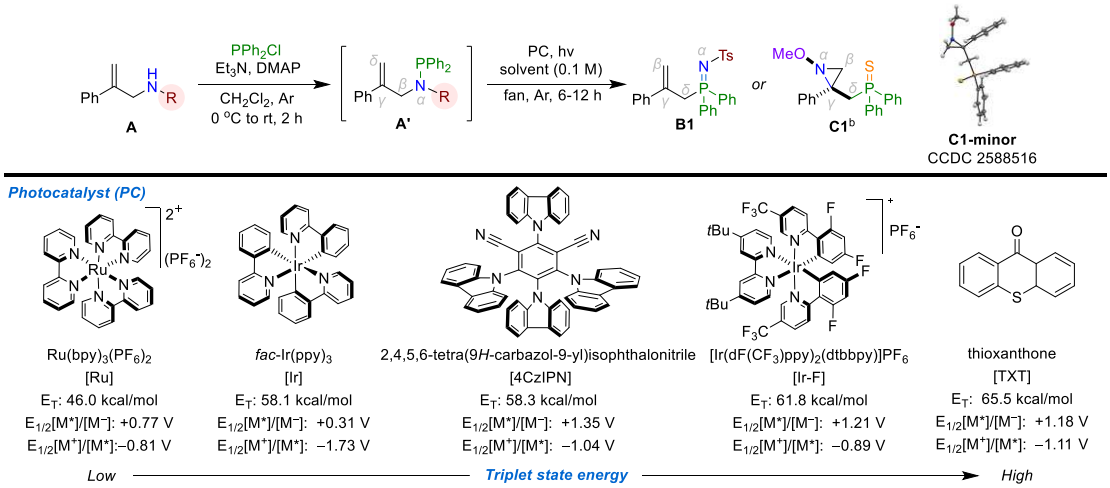
Results and discussion

Reaction conditions optimization

The study began with a one-pot reaction of N-substituted-2-phenylprop-2-en-1-amine **A** with Ph_2PCl in CH_2Cl_2 in the presence of Et_3N and DMAP, followed by an EnT process catalyzed by $[Ir(dF(CF_3)ppy)_2(dtbbpy)]PF_6$ (Ir-F) under blue LED irradiation (455 nm, 6 W), as shown in Table 1. Initially, electron-withdrawing groups (EWGs) such as acyl and benzoyl were installed as the *N*-substituent. However, only the corresponding aminophosphine intermediates **A'** were formed in situ, but no subsequent photocatalytic rearrangement occurred (Table 1, entries 1 and 2). To our delight, when another EWG, tosyl, was employed as the N-substituent, the desired rearrangement reaction proceeded smoothly, affording N-tosyl diphenyl(2-phenylallyl)-λ^5-phosphanimine **B1** in 81% yield (Table 1, entry 3). Other photocatalysts with high triplet-state energy (TSE), such as thioxanthone (TXT), 2,4,5,6-tetra(9H-carbazol-9-yl)isophthalonitrile (4CzIPN), and *fac*-$Ir(ppy)_3$ (Ir), also delivered the desired **B1** in 73%, 64%, and 43% yields, respectively; while $Ru(bpy)_3(PF_6)_2$ (Ru) with a markedly low TSE, was ineffective for the reaction (Table 1, entries 4-7). Solvent screening

indicated that CH_2Cl_2 outperformed EtOAc and MeCN (Table 1, entries 8 and 9). Notably, replacing tosyl-substituent by a methoxy group, an electron-donating group (EDG), completely switched the reaction outcome: the corresponding product **B** was not detected, and only the phosphine-tethered N-methoxy aziridine was generated. Upon workup with elemental sulfur S_8, this species was isolated as stable adduct **C1** in 52% yield (Table 1, entry 10). Further solvent optimization raised the yield of **C1** to 78% when EtOAc was used as the reaction medium (Table 1, entries 11 and 12). Nevertheless, other EDGs such as alkyl and aryl groups proved inert under these conditions, yielding neither **C** nor **B** (Table 1, entries 13 and 14).

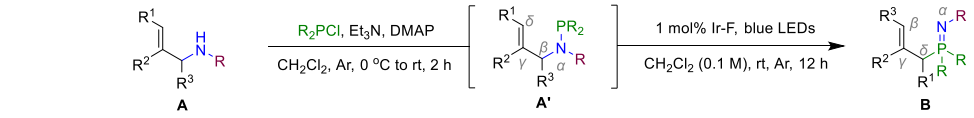
Table 1 Exploration and Optimization



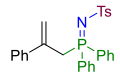
entry	R	photocatalyst	solvent	yield (%)[a]	
				B	**C**
1	Ac	Ir-F	CH_2Cl_2	NR	NR
2	Bz	Ir-F	CH_2Cl_2	NR	NR
3	Ts	Ir-F	CH_2Cl_2	**B1**, 81	0
4	Ts	TXT	CH_2Cl_2	**B1**, 73	0
5	Ts	4CzIPN	CH_2Cl_2	**B1**, 64	0
6	Ts	*fac*-Ir(ppy)$_3$	CH_2Cl_2	**B1**, 43	**0**
7	Ts	Ru(bpy)$_3$(PF$_6$)$_2$	CH_2Cl_2	NR	NR
8	Ts	Ir-F	AcOEt	**B1**, 68	0
9	Ts	Ir-F	MeCN	**B1**, 66	0
10	MeO	Ir-F	CH_2Cl_2	0	**C1**, 52, dr 2.3:1[c]
11	MeO	Ir-F	EtOAc	0	**C1**, 78, dr 2.5:1[c]
12	MeO	Ir-F	MeCN	0	**C1**, 67, dr 2.0:1[c]
13	*n*Bu	Ir-F	CH_2Cl_2	NR	NR
14	Ph	Ir-F	CH_2Cl_2	NR	NR

[a]Standard conditions: **A** (0.2 mmol), DMAP (20 mol%), Et_3N (1.2 equiv.), and Ph_2PCl (1.2 equiv.) in dry DCM (2 mL) were stirred at 0 °C to room temperature under argon for 2 h. Ir-F (1.0 mol%) was then added and the mixture was stirred under Ar with blue LEDs (455 nm, 6 W) irradiation for 12 h. Isolated yields. [b]After work-up with S_8 in situ. [c]Diastereomer ratios were determined by ^{1}H NMR.

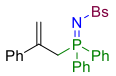
Table 2. *N*-Sulphonyl-Mediated *β*-Scission Rearrangement of Aminophosphine[a]



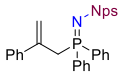
Variation of N-sulphonyls



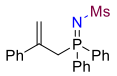
B1, 81%



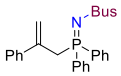
B2, 76%



B3, 61%

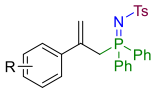


B4, 75%



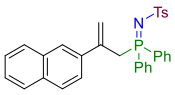
B5, 79%

Variation of alkenes

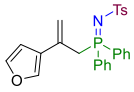


B6, 77%

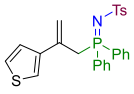
B6, R = OMe, 61%
B7, R = Me, 77%
B8, R = CN, 65%
B9, R = *m*-Me, 49%



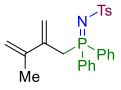
B10, 51%



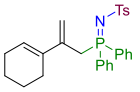
B11, 48%



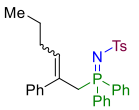
B12, 55%



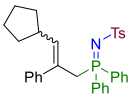
B13, 46%



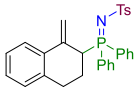
B14, 53%



B15, 75%, E/Z 1:1[b]

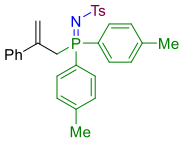


B16, 71%, E/Z 5:1[b]

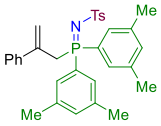


B17, 52%

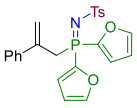
Variation of R_2PCl



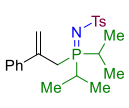
B18, 63%



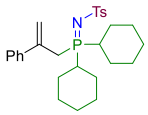
B19, 61%



B20, 44%



B21, 41%



B22, 36%

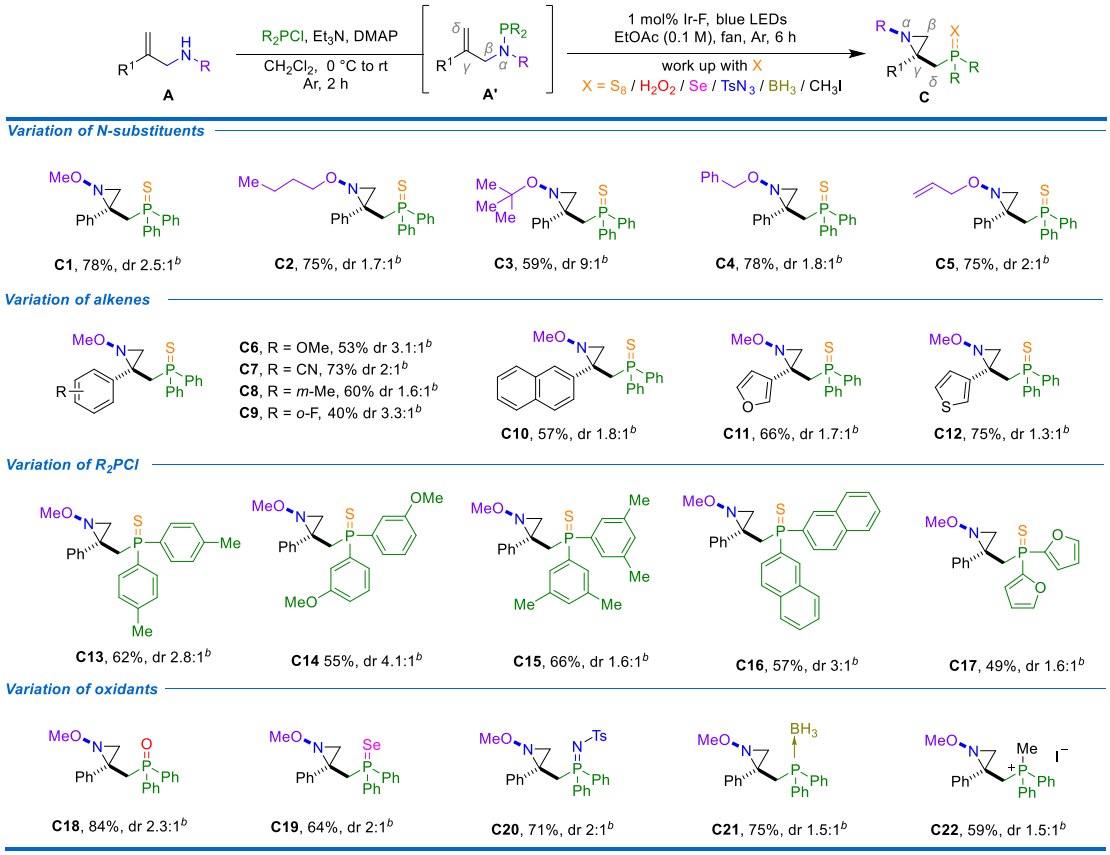
[a]Standard conditions: **A** (0.2 mmol), DMAP (20 mol%), Et_3N (1.2 equiv.), and R_2PCl (1.2 equiv.) in dry DCM (2 mL) were stirred at 0 °C to room temperature under Ar for 2 h. Ir-F (1.0 mol%) was then added and the mixture was stirred under Ar with blue LEDs (455 nm, 6 W) irradiation for 12 h. Isolated yields are given. [b]Z/E ratios of alkenes were determined by ^1H NMR.

Reaction scope

With the optimal conditions in hand, we explored the substrate scope of this dichotomous diradical rearrangement. We first investigated the N-sulfonyl-tuned β-scission-mediated rearrangement, and the corresponding results are summarized in Table 2. N-Sulphonyl examination revealed that in addition to tosyl, other sulphonyl groups such as benzenesulfonyl (Bs), 2-naphthalenesulfonyl (Nps), methanesulfonyl (Ms), and butanesulfonyl (Bus)-incorporated substrates **A** were all suitable for this conversion, delivering the corresponding *N*-sulphonyl diphenyl(2-phenylallyl)-λ^5-phosphanimine products **B2-B5** in good yields. The reaction scope was further tested by variation of the alkene moiety. Substrates bearing 2-phenylprop-2-enyl with *para*-substituents of diverse electronic properties on the phenyl ring, such as MeO, Me, and CN, all participated very well in the reaction, giving rise to the desired products **B6-B8** in good yield. Besides, the meta-substituted 2-phenylprop-2-enyl transformed very well in the protocol and gave the desired products **B9** in 49% yield. In addition, naphthalene ethylene with a large conjugated π-system and sensitivity to EnT process was also a good candidate in this transformation, generating the corresponding product **B10** in 51% yield. Besides aryl vinyl substrates, heteroaryl such as furan and thiophene also afforded the desired products **B11** and **B12** in 48% and 55% yields, respectively. Conjugated alkenes such as 3-methylbuta-1,3-dien-2-yl and 1-cyclohexenyl-1-vinyl were also good reaction partners, producing the corresponding products **B13** and **B14** in 46% and 53% yields, respectively. Notably, when the

reaction involved terminal alkenes with substituents such as propyl and cyclopentyl at the methylene moiety, this rearrangement took placed very well and provided λ^5-phosphanimine internal alkenes **B15** and **B16** in good yields with a E/Z ratio of approximately 1:1 and 5:1. When internal alkenes such as the cyclohexenyl incorporated substrate was employed, the corresponding rearrangement generated the terminal alkenes, as demonstrated in the case of **B17**. Moreover, in addition to Ph_2PCl, chlorodiphenylphosphines bearing *para*- or *meta*-substituents on the benzene ring can also engage in this reaction to afford the corresponding products **B18** and **B19** in 63% and 61% yields, respectively. Heteroaryl-substituted phosphines, such as chlorodifurylphosphine also afforded the desired product **B20** in 44% yield. Significantly, dialkylchlorophosphines such as diisopropylchlorophosphine and dicyclohexylchlorophosphine are amenable to this synthetic strategy too, furnishing **B21** and **B22** in moderate yields.

Table 3. *N*-Alkoxyl-Mediated *α*-Scission Rearrangement of Aminophosphine[a]



[a]Standard conditions: **A** (0.2 mmol), DMAP (20 mol%), Et_3N (1.2 equiv.), and R_2PCl (1.2 equiv.) in dry DCM (2 mL) were stirred from 0 °C to room temperature under Ar for 2 h. After removal of CH_2Cl_2, Ir-F (1.0 mol%) and EtOAc (2 mL) were added, and the mixture was stirred under Ar upon with blue LEDs (455 nm, 6 W) irradiation with fan-cooling. Upon full consumption of intermediate **A'**, the reaction mixture was treated in situ with S_8, H_2O_2, Se, TsN_3, $Me_2S{\bullet}BH_3$ or CH_3I, respectively. Isolated yields are given. [b]Diastereomeric ratios were determined by ^1H NMR.

Having successfully achieved N-sulphonyl-mediated diradical *β*-scission rearrangement of aminophosphines, we next explored the scope of its *α*-scission counterpart contolled by N-alkoxyl groups, with the results illustrated in Table 3. It can be clearly seen that, besides methoxy, substrates decorated with various N-alkoxyl moieties, such as *n*-butyloxy (O*n*Bu), *t*-butyloxy (O*t*Bu),

benzyloxy (OBn), and allyloxy (Oallyl), were all compatible with this conversion, delivering the corresponding thiophosphoryl-functionalized N-alkoxyl aziridine **C2-C5** in good yields. 2-Phenylprop-2-enyl substrates bearing para-phenyl substituents of divergent electronic characters, such as MeO and CN, were well tolerated under standard conditions, affording the desired products **C6** and **C7** in 53% and 73% yields, respectively. Likewise, *meta*-methyl and *ortho*-fluoro-substituted 2-phenylprop-2-enyl substrates were also good reaction partner and afforded **C8** and **C9** in 60% and 40% yields, respectively. We further expanded the substrate scope to naphthyl- and heteroaryl-substituted alkenes. Alkenes incorporating 2-naphthyl-, 3-furyl-, and 3-thienyl groups readily underwent this reaction, giving products **C10-C12** in good yields. Moreover, in addition to Ph_2PCl, chlorodiphenylphosphines with para- or meta-substituents on the phenyl rings also performed well in this protocol, providing compounds **C13-C15** in good yields. Gratifyingly, chlorodi(2-naphthyl)phosphine and chlorodi(2-furyl)phosphine also reacted efficiently to afford **C16** and **C17.** To showcase the synthetic utility of this approach, the resulting phosphine intermediates were subjected to diverse post-functionalization manipulations including oxygenation by H_2O_2, selenium insertion, azidation with TsN_3, borane complexation with $BH_3{\cdot}SMe_2$, and quaternization with CH_3I. All these derivations proceeded smoothly to furnish products **C18**–**C22** in good to excellent yields. Collectively, these outcomes demonstrate the broad applicability and considerable synthetic potential of this strategy toward structurally diverse organophosphorus frameworks.

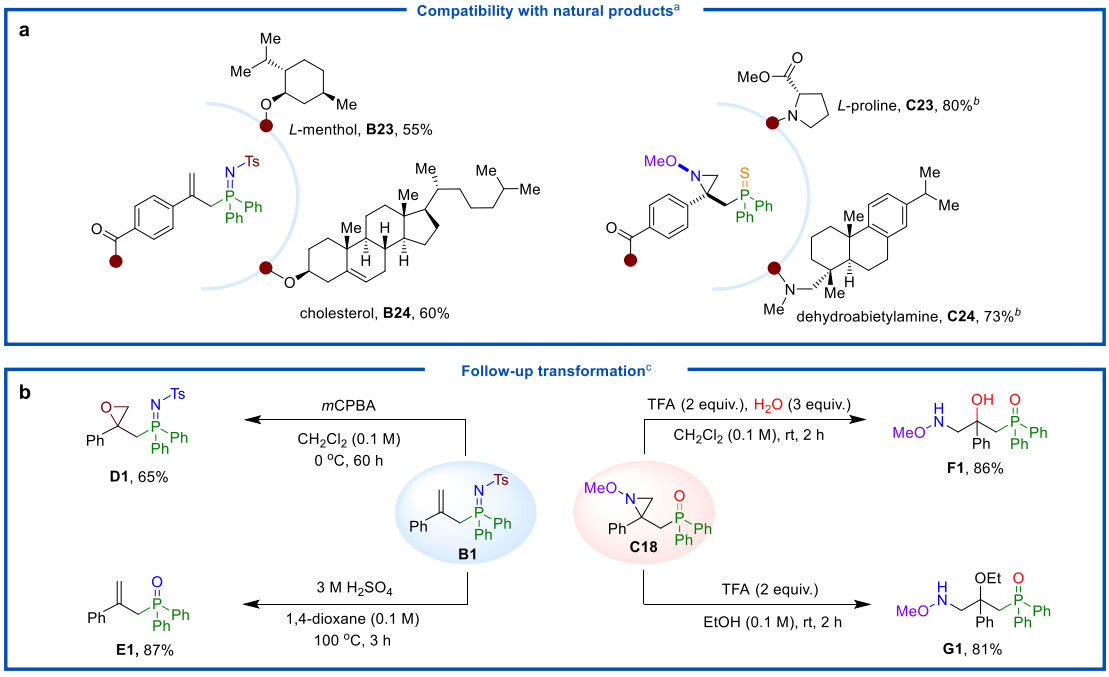


Figure 2. Reaction Compatibility and Follow-up Transformation. (**a**) Compatibility with natural products. [a]Standard conditions. [b]Product was obtained as a mixture of diastereomers (see Supplementary Information (SI) for detail). Isolated yields are given. (**b**) Follow-up transformation. [c]**B1** or **C18** (0.2 mmol), see SI for detail.

To demonstrate the generality and practical utility of this method, the photocatalytic aminophosphine rearrangement was applied to a range of natural products and drug derivatives (Figure 2a). Gratifyingly, substrates derived from *L*-menthol and cholesterol smoothly underwent

β-scission rearrangement of the aminophosphine moiety, affording products **B23** and **B24** in 55% and 60% yields, respectively. Furthermore, *L*-proline- and dehydroabietylamine-derived substrates also exhibited excellent reactivity toward *α*-scission rearrangement, delivering compounds **C23** and **C24** in 73% and 80% yields, respectively. To further demonstrate the synthetic utility of this method, a set of downstream transformations were performed (Figure 2b). Epoxidation of the C=C double bond in **B1** with *m*CPBA delivered **D1** in 65% yield, while hydrolysis of the imine moiety in **B1** with 3 M H_2SO_4 gave **E1** in 87% yield. In addition, under trifluoroacetic acid (TFA) promotion, ring-opening nucleophilic substitution of phosphoryl-featured aziridine **C18** with H_2O furnished **F1** in 86% yield, while ethanolysis with EtOH yielded **G1** in 81% yield via selective C–O bond formation.

To reveal the mechanistic details of this transformation, a set of control experiments were carried out (Figure 3a). When 2,2,6,6-tetramethylpiperidin-1-oxyl (TEMPO), a carbon-radical scavenger, was introduced into the model reactions of **A′1-Ts** and **A′1-OMe** under standard conditions, both reactions were fully suppressed, and no desired products **B1** and **C′1** could be detected. Comparable inhibitory effects were also observed upon addition of the triplet quencher 2,5-dimethylhexa-2,4-diene to these model reactions. Furthermore, upon direct irradiation with purple LEDs (365 nm, 6 W) in the absence of photocatalyst, the model reactions still afforded **B1** and **C′1** in 26% and 28% yields, respectively. Collectively, these observations corroborate that the rearrangement proceeds via a triplet diradical pathway. UV-vis absorption measurements of **A′1-OMe**, **A′1-Ts** and the Ir-F photocatalyst demonstrate that only Ir-F exhibits intense absorption at 450 nm, which supports a triplet-triplet energy-transfer mechanism for this transformation (see supplementary information for UV-vis absorption).

To elucidate the mechanistic origin of N-substituent-tuned selective radical α- or β-scission in this phosphanamine rearrangement, density functional theory (DFT) calculations were performed using **A′1-OMe** and **A′1-Ts** as model substrates (Figure 3b-d). First, the triplet energy of **A′1-OMe** was calculated to be 48.8 kcal mol^{-1}, which falls within the EnT sensitization range for typical organic photosensitizers and thus validates the feasibility of visible-light EnT. Photosensitization generates the triplet excited state ^{3}**A′1-OMe**, which undergoes carbon-radical mediated cyclization onto the P (III)-atom via **TS1-OMe** ($\Delta G^{\ddagger}$ = 6.4 kcal mol^{-1}) to furnish the key phosphoranyl-based triplet diradical intermediate **INT1-OMe**. From **INT1-OMe**, N-P bond cleavage proceeds through **TS2** with a low barrier of 8.7 kcal mol^{-1}, yielding the 1,3-triplet N,C-diradical **INT2**. In sharp contrast, the competing C-N bond cleavage via **TS2′** is kinetically prohibitive ($\Delta G^{\ddagger}$ = 23.2 kcal mol^{-1}) and fails to produce the 1,2-triplet diradical **INT2′**. The favorable **INT2** intermediate subsequently undergoes intersystem crossing (ISC) to the singlet state, followed by intramolecular radical-radical coupling across the N- and C-centered radical sites to deliver the final aziridine product **C′1**.

For **A'1-Ts**, EnT-promoted photosensitization generates the triplet excited state ^{3}**A'1-Ts**, which undergoes carbon radical-mediated cyclization onto the P(III) center via **TS1-Ts** ($\Delta G^{\ddagger}$ = 4.9 kcal mol^{-1}) to furnish **INT1-Ts**. Subsequent C–N bond cleavage through **TS3** demands an activation free energy of 22.4 kcal mol^{-1}, while N–P bond cleavage via **TS3'** proceeds with a lower barrier of 17.0 kcal mol^{-1}. Notably, the α-/β-scission selectivity predicted by these energy barriers contradicts the experimental observations, motivating us to search for alternative pathways that can account for the experimental selectivity. Given the biradical character of **INT1-Ts**, we envisioned a fragmentation channel engaging both radical sites, analogous to 1,4-biradical cleavage in Norrish type II reactions.[59,60] This mechanistic manifold differs fundamentally from conventional radical

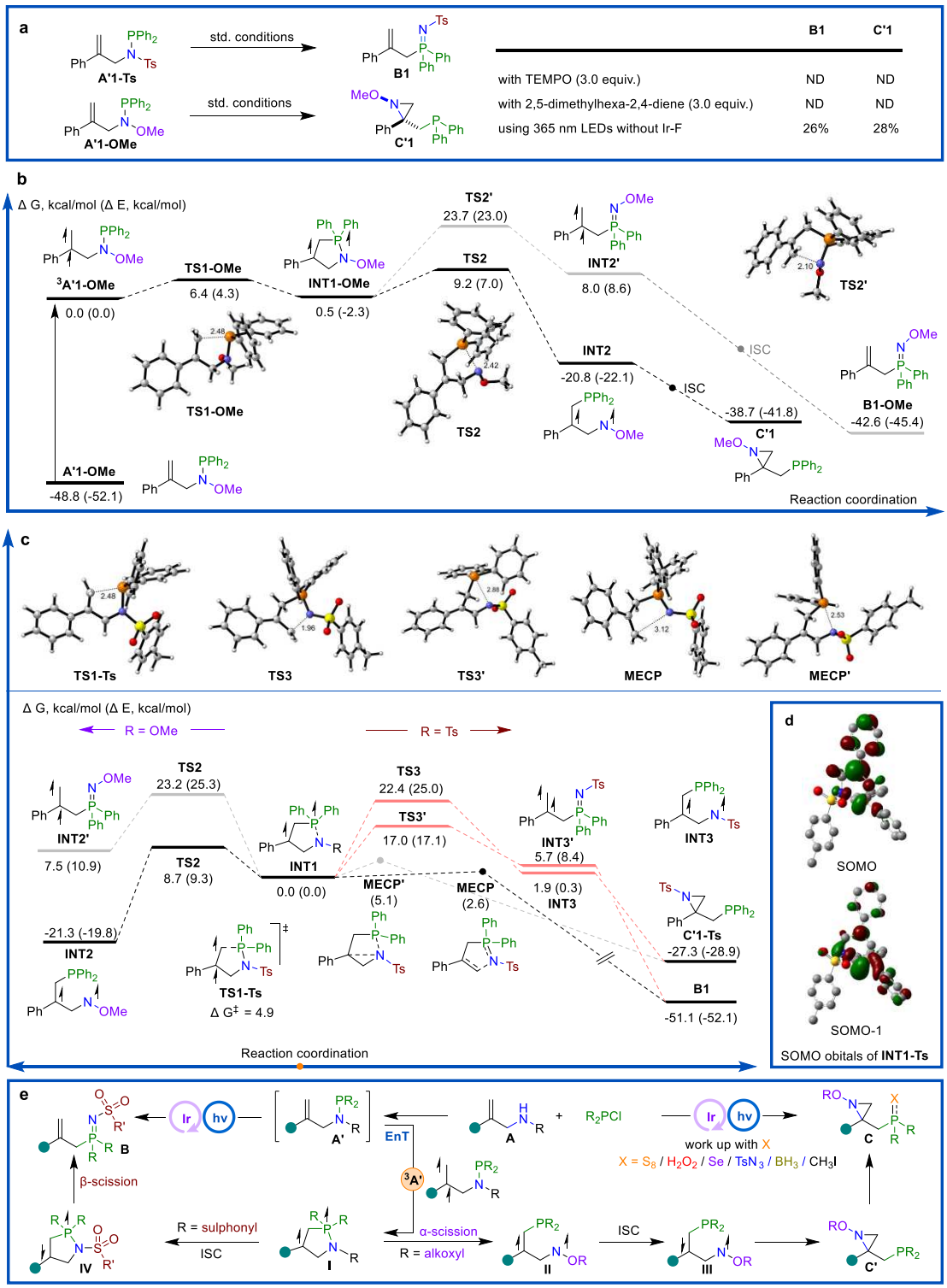


Figure 3. Mechanistic Investigations and Proposed Mechanism. (**a**) radical-inhibition and triplet quenching experiments. (b) Calculated energy profile for the α-scission pathway. (c) Calculated energy profile for the β-scission pathway and energy comparison between α- and β-scission processes. (d) Calculated SOMO orbitals of intermediate **INT1-Ts**. (e) Proposed Mechanism. All DFT calculations were performed using Gaussian 16 at the SMD(EtOAc)-B3LYP-D3/6-311+G(d,p)//B3LYP/6-31+G(d,p) theoretical level.

rearrangements. Following this hypothesis, we identified a minimum-energy crossing point (**MECP**, $\Delta E = 2.6$ kcal mol^{-1}) linking the triplet potential-energy surface of **INT1-Ts** to the singlet surface that yields **B1**. An alternative pathway toward **C′1-Ts** via N–P bond cleavage was also evaluated, which proceeds through a higher-energy **MECP′** ($\Delta E = 5.1$ kcal mol^{-1}). These computational findings indicate that the triplet-to-singlet ISC pathway leading to **B1** is energetically preferred. Orbital analysis for the SOMO and SOMO-1 of the triplet biradical **INT1-Ts** shows parallel p-orbital alignment at the carbon- and phosphorus-centered radical sites (Figure 3d). This orbital arrangement further corroborates the feasibility of the Norrish type II-like 1,4-biradical fragmentation. On the basis of the aforementioned studies, a plausible reaction mechanism is depicted in Figure 3e. In-situ condensation of amines **A** with R_2PCl under basic conditions affords aminophosphines **A′**. Visible light-mediated EnT populates the triplet excited state ^{3}**A′** via sensitization of the vinyl moiety of **A′**. This species undergoes fast radical cyclization, where the terminal carbon radical attacks the P(III) center, generating phosphoranyl-based triplet diradical intermediates **I**. Driven by the electronic nature of the N-substituent, intermediates **I** undergo selective α- or β-scission of the phosphoranyl radical. For N-alkoxy-substituted **I**, α-scission occurs to furnish triplet 1,3-C,N-diradical **II**. Subsequent ISC of **II** delivers singlet diradical **III**, which collapses to give N-alkoxy aziridine **C′**. Further in-situ derivatization of **C′** using with S_8, H_2O_2, selenium powder, TsN_3, BH_3•SMe_2, or CH_3I yields the final products **C**. In contrast, N-sulfonyl-substituted **I** proceeds via ISC to generate phosphoranyl-based singlet diradical intermediates **IV**, which then undergo Norrish type II-like 1,4-diradical fragmentation to afford N-sulfonyl allyl-λ^5-phosphanimines **B**.

Conclusion

In summary, this study establishes a mild visible-light energy transfer photocatalytic protocol that enables divergent fragmentation of in situ generated aminophosphoranyl radicals using readily accessible amines and chlorophosphines as starting materials. Simply tuning the N-substituent allows precise switching of the radical cleavage pathway, effectively addressing the inherent limitation of fragmentation selectivity control in radical chemistry. Specifically, N-alkoxy substituents favor α-scission to furnish phosphine-featured aziridine skeletons, whereas N-sulfonyl substituents trigger Norrish type II-like 1,4-diradical β-fragmentation to yield λ^5-phosphanimine products. DFT calculations demonstrate that the electronic properties of N-substituents govern product selectivity by modulating the geometric configuration and orbital alignment of phosphoranyl radicals. The resulting phosphine-featured aziridine and λ^5-phosphanimine frameworks serve as versatile organophosphorus building blocks that tolerate diverse downstream functionalizations. Featuring broad substrate compatibility, tunable product scaffold, and high step economy, this modular and practical strategy provides a facile platform for the construction of structurally diverse organophosphorus compounds.

■ ASSOCIATED CONTENT

• Data Availability Statement

The data underlying this study are available in the published article and its Supplementary Information.

• Supplementary Information Statement

Supplementary information accompanies this paper. It contains experimental procedures, spectral characterization, crystallographic data, and DFT calculations (PDF).

• Accession Codes

Deposition numbers 2588516 (for **C1-minor**) contain the supplementary crystallographic data for this paper. These data are provided free of charge by the joint Cambridge Crystallographic Data Centre and Fachinformationszentrum Karlsruhe Access Structures service.

■ ACKNOWLEDGMENTS

We thank the National Natural Science Foundation of China (No. 22471109 and 22171118) and the Science and Technology Major Program of Gansu Province of China (23ZDFA015 and 24ZD13FA017) for financial support, and the Supercomputing Center of Lanzhou University for providing the computational resources for the DFT calculations.

■ AUTHOR CONTRIBUTIONS

B.H. conceived and directed the project. P.Z., H.C. and L.X. performed experiments. P.Z., Z.W., H.C. and L.X. prepared the Supplementary Information. Z.W. performed the DFT calculations. B.H., P.Z. and Z.W. wrote the paper. All authors discussed the results and commented on the manuscript.

Notes

The authors declare no competing financial interests.

■ REFERENCES

1. Studer, A. & Curran, D. P. Catalysis of radical reactions: a radical chemistry perspective. *Angew. Chem. Int. Ed.* **55**, 58–102 (2016).
2. Yan, M., Lo, J. C., Edwards, J. T. & Baran, P. S. Radicals: reactive intermediates with translational potential. *J. Am. Chem. Soc.* **138**, 12692–12714 (2016).
3. Ishibashi, H. Controlling the regiochemistry of radical cyclizations. *Chem. Rec.* **6**, 23–31 (2006).
4. Hoffmann, R. W. Markovnikov free radical addition reactions, a sleeping beauty kissed to life. *Chem. Soc. Rev.* **45**, 577–583 (2016).
5. Gilmore, K., Mohamed, R. K. & Alabugin, I. V. The Baldwin rules: revised and extended. *WIREs Comput. Mol. Sci.* **6**, 487–514 (2016).
6. Zhu, Z., Zhang, Y., Li, Z. & Shu, C. Photoinduced radical-polar crossover cyclization reactions. *Chem Catal.* **4**, 100945 (2024).
7. Cao, G.-M. et al. Navigating the functionalization of unactivated alkenes via visible light photocatalysis. *Chem. Soc. Rev.* **54**, 6726–6806 (2025).
8. Wu, X., Ma, Z., Feng, T. & Zhu, C. Radical-mediated rearrangements: past, present, and future. *Chem. Soc. Rev.* **50**, 11577–11613 (2021).
9. Zhao, G., Mukherjee, U., Yao, W. & Ngai, M.-Y. Catalytic 1,2-radical acyloxy migration: a strategy to access novel chemical space and reaction profiles. *Acc. Chem. Res.* **58**, 1815–1829 (2025).
10. Chen, J.-J., Chen, S.-S., Wang, Q.-Z. & Huang, H.-M. Recent advances in photochemical rearrangements involving diradicals. *Chem. Soc. Rev.* **55**, 6221–6256 (2026).
11. Wei, D. Liu, T., He, Y. et al. Radical 1,4/5-amino shift enables access to fluoroalkyl-containing primary β(γ)-aminoketones under metal-free conditions. *Angew. Chem. Int. Ed.* **60**, 26308–26313 (2021).

12. Chen, K. et al. Functional-group translocation of cyano groups by reversible C–H sampling. *Nature* **620**, 1007–1012 (2023).
13. Hu, S.-P., Gao, C.-H., Liu, T.-M. et al. Integrating olefin carboamination and Hofmann–Löffler–Freytag reaction by radical deconstruction of hydrazonyl N–N bond. *Angew. Chem. Int. Ed.* **63**, e202400168 (2024).
14. Zhang, W., Mao, S., Peng, M. & Xi, Y. Positional editing of diverse functional groups through radical 1,2-boron shifts. *Nat. Synth.* **5**, 1021–1031 (2026).
15. Zhang, Z., Qian, X., Gu, Y. & Gui, J. Controllable skeletal reorganizations in natural product synthesis. *Nat. Prod. Rep.* **41**, 251–272 (2024).
16. Li, L., Li, Z.-L., Gu, Q.-S., Wang, N. & Liu, X.-Y. A remote C–C bond cleavage-enabled skeletal reorganization: access to medium-/large-sized cyclic alkenes. *Sci. Adv.* **3**, e1701487 (2017).
17. Wu, L. et al. Photocatalyzed epimerization of quaternary stereocenters. *J. Am. Chem. Soc.* **147**, 11080–11088 (2025).
18. Cheng, Z., Huang, K., Wang, C. et al. Catalytic remodeling of complex alkenes to oxonitriles through C=C double bond deconstruction. *Science* **387**, 1083–1090 (2025).
19. Bao, F.-S. et al. Photocatalytic conversion of aminocyclopropanes to γ-lactams by sequential ring-expansion and peripheral diversification. *J. Am. Chem. Soc.* **148**, 31032–31042 (2026).
20. Justicia, J. & Morcillo, S. P. Radical-promoted "unstrained" C–C and C–N bond cleavage: a blueprint for deconstructive skeletal editing. *Chem. Soc. Rev.* **55**, 7438–7464 (2026).
21. Chang, L., An, Q., Duan, L., Feng, K. & Zuo, Z. Alkoxy radicals see the light: new paradigms of photochemical synthesis. *Chem. Rev.* **122**, 2429–2486 (2022).
22. Lai, S.-Q., Wei, B.-Y., Wang, J.-W., Yu, W. & Han, B. Photocatalytic anti-Markovnikov radical hydro- and aminooxygenation of unactivated alkenes tuned by ketoxime carbonates. *Angew. Chem. Int. Ed.* **60**, 21997–22003 (2021).
23. Zhang, Z. Lonardi, G., Sephton, T. et al. Deaminative cross-coupling of amines by boryl radical β-scission. *Nature* **647**, 913–921 (2025).
24. Peng, P., Roure, B., Lulli, T. et al. Divergent Ring Opening and Functionalization of N-Alkyl Aziridines via Boryl Radical Fragmentation. *Nat. Chem.* 2026. https://doi.org/10.1038/s41557-026-02247-x.
25. Zhang, Y., Zhou, G., Liu, S. & Shen, X. Radical Brook rearrangement: past, present, and future. *Chem. Soc. Rev.* **54**, 1870–1904 (2025).
26. Li, B., He, X., Zhang, Y. et al. Hydroxyl radicals unlock strong C(sp3)–Si bonds: photocatalytic alkylation and silacycle engineering. *Angew. Chem. Int. Ed.* **65**, e202523587 (2026).
27. Rossi-Ashton, J. A., Clarke, A. K., Unsworth, W. P. & Taylor, R. J. K. Phosphoranyl radical fragmentation reactions driven by photoredox catalysis. *ACS Catal.* **10**, 7250–7261 (2020).
28. Bentrude, W. G. Phosphoranyl radicals: their structure, formation, and reactions. *Acc. Chem. Res.* **15**, 117–125 (1982).
29. Bentrude, W. G., Hansen, E. R., Khan, W. A. & Rogers, P. E. α vs β scission in reactions of alkoxy and thiyl radicals with diethyl alkylphosphonites. *J. Am. Chem. Soc.* **94**, 2867–2868 (1972).
30. Hay, R. S., Roberts, B. P., Singh, K. & Wilkinson, J. P. T. Electron spin resonance studies of radicals derived from trialkyl phosphorimidates, (RO)3P=NR. Phosphazene formation by β-scission of an aminophosphoranyl radical. *J. Chem. Soc., Perkin Trans. 2* 756–762 (1979).
31. Masuda, Y. et al. Photocatalytic 1,2-phosphorus-migrative [3+2] cycloaddition of tri(t-butyl)phosphine with terminal alkynes. *J. Am. Chem. Soc.* **145**, 19060–19066 (2023).
32. Wang, J., Zhang, Y., Zhu, L., Xue, X.-S. & Li, C. Photoinduced remote C(sp3)–H phosphonylation of amides. *Angew. Chem. Int. Ed.* **63**, e202400856 (2024).

33. Bissonnette, N. B., Bisballe, N., Tran, A. V., Rossi-Ashton, J. A. & MacMillan, D. W. C. Development of a general organophosphorus radical trap: deoxyphosphonylation of alcohols. *J. Am. Chem. Soc.* **146**, 7942–7949 (2024).

34. Lin, X., Fei, H., Zhang, Z. et al. Cobalt-catalyzed Markovnikov-selective hydrophosphorylation of unactivated alkenes enabled by phthalimidyl phosphite reagents. *Nat. Commun.* 2026. https://doi.org/10.1038/s41467-026-77482-4.

35. Li, K.-D., Tang, Y.-H. & Huang, H.-M. Redirecting radical phosphonylation via energy-transfer-enabled diradical rearrangement. *Sci. Adv.* **12**, eaee4031 (2026).

36. Zhang, M., Xie, J. & Zhu, C. A general deoxygenation approach for synthesis of ketones from aromatic carboxylic acids and alkenes. *Nat. Commun.* **9**, 3517 (2018).

37. Li, Y. Shao, Q., He, H. et al. Highly selective synthesis of all-carbon tetrasubstituted alkenes by deoxygenative alkenylation of carboxylic acids. *Nat. Commun.* **13**, 10 (2022).

38. Zhang, J., Mück-Lichtenfeld, C. & Studer, A. Photocatalytic phosphine-mediated water activation for radical hydrogenation. *Nature* **619**, 506–513 (2023).

39. Xu, W., Fan, C., Hu, X. & Xu, T. Deoxygenative transformation of alcohols via phosphoranyl radical from exogenous radical addition. *Angew. Chem. Int. Ed.* **63**, e202401575 (2024).

40. Chinn, A. J., Sedillo, K. & Doyle, A. G. Phosphine/photoredox catalyzed anti-Markovnikov hydroamination of olefins with primary sulfonamides via α-scission from phosphoranyl radicals. *J. Am. Chem. Soc.* **143**, 18331–18338 (2021).

41. Kim, J., Kim, M., Jeong, J. & Hong, S. Unlocking the potential of β-fragmentation of aminophosphoranyl radicals for sulfonyl radical reactions. *J. Am. Chem. Soc.* **145**, 14510–14518 (2023).

42. Wearing, E. R., Kaushik, N. P., Hugie, S. T., Sigman, M. S. & Doyle, A. G. Origin of scission selectivity for phosphoranyl radicals in photoredox catalysis. *J. Am. Chem. Soc.* **148**, 37121–37133 (2026).

43. Xie, D.-T., Chen, H.-L., Wei, D. et al. Regioselective fluoroalkylphosphorylation of unactivated alkenes by radical-mediated alkoxyphosphine rearrangement. *Angew. Chem. Int. Ed.* **61**, e202203398 (2022).

44. Li, Y.-F., Wang, H.-C. & Han, B. Catalytic Markovnikov hydrophosphorylation of unactivated olefins via a radical-polar crossover rearrangement. *Nat. Commun.* **17**, 6500 (2026).

45. Strieth-Kalthoff, F., James, M. J., Teders, M., Pitzer, L. & Glorius, F. Energy transfer catalysis mediated by visible light: principles, applications, directions. *Chem. Soc. Rev.* **47**, 7190–7202 (2018).

46. Zhou, Q.-Q., Zou, Y.-Q., Lu, L.-Q. & Xiao, W.-J. Visible-light-induced organic photochemical reactions through energy-transfer pathways. *Angew. Chem. Int. Ed.* **58**, 1586–1604 (2019).

47. Lee, D. S., Soni, V. K. & Cho, E. J. N–O bond activation by energy transfer photocatalysis. *Acc. Chem. Res.* **55**, 2526–2541 (2022).

48. Mao, B., Yan, J., Wei, Y. & Shi, M. Hydrogen atom transfer promoted by carbon-centered biradicals via energy transfer catalysis. *Acc. Chem. Res.* **58**, 2028–2045 (2025).

49. Lee, W., Koo, Y., Jung, H., Chang, S. & Hong, S. Energy-transfer-induced [3+2] cycloadditions of N–N pyridinium ylides. *Nat. Chem.* **15**, 1091–1099 (2023).

50. Liu, T.-M. Zhu, L.-Y., Qi, M.-H. et al. Photosensitized diradical rearrangement of alkenyl oxime ethers towards amino-featured oxiranes: reaction, mechanism, and structural prediction. *Chem. Sci.* **16**, 14811–14821 (2025).

51. Lai, S.-Q., Zhao, P.-F., Wang, Z.-S. et al. Conversion of alkenes into simple or functionalized aldehydes by reaction with an ambiphilic masked formyl radical. *Angew. Chem. Int. Ed.* **65**, e6695860 (2026).

52. Zhang, F., Domack, J., Hölter, N., Daniliuc, C. G. & Glorius, F. Divergent housane synthesis via intramolecular [2+2] cycloaddition of 1,4-dienes. *Nat. Synth.* **5**, 897–906 (2026).

53. Zhang, Z.-X. Shu, K., Popescu, M. V. et al. Programmable regiodivergent light-driven cyclization of acyclic 1,5-dienes unlocks rigid bicyclic architectures. *Nat. Chem.* https://doi.org/10.1038/s41557-026-02238-y (2026).

54. Cooper, J. W., Roberts, B. P. Configurational Effects in the α-Scission of Phosphoranyl Radicals. *J. Chem. Soc., Perkin Trans. 2* **5**, 808–813 (1976).

55. Roberts, B. P., Singh, K. Site Selectivity in the β-Scission of Alkoxophosphoranyl Radicals. A Reinterpretation. *J. Chem. Soc., Perkin Trans. 2* **9**, 1549–1556 (1980).

56. Romanenko, V. D. & Kukhar, V. P. Fluorinated phosphonates: synthesis and biomedical application. *Chem. Rev.* **106**, 3868–3935 (2006).

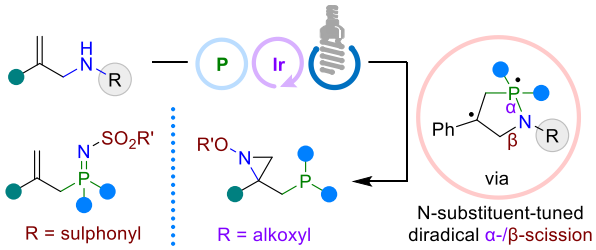
57. Priegert, A. M., Rawe, B. W., Serin, S. C. & Gates, D. P. Polymers and the p-block elements. *Chem. Soc. Rev.* **45**, 922–953 (2016).

58. Guo, H., Fan, Y. C., Sun, Z., Wu, Y. & Kwon, O. Phosphine organocatalysis. *Chem. Rev.* **118**, 10049–10293 (2018).

59. Wagner, P. J. & Klán, P. Norrish type II photoelimination of ketones: cleavage of 1,4-biradicals formed by γ-hydrogen abstraction. in *CRC Handbook of Organic Photochemistry and Photobiology* 2nd edn, Ch. 52 (eds. Horspool, W. M. & Lenci, F.) 52-1–52-34 (CRC Press, Boca Raton, FL, 2004).

60. He, H.-Y. & Fang, W.-H. Photochemistry of butyrophenone: combined complete-active-space self-consistent field and density functional theory study of Norrish type I and II reactions. *J. Phys. Chem. A* **108**, 5386–5392 (2004).

Insert Table of Contents artwork here



Supplementary Files

This is a list of supplementary files associated with this preprint. Click to download.

- SI20261024.pdf